

FREE ELECTRON IN COMPRESSED INERT GASES

E. B. Gordon^{a*}, *B. M. Smirnov*^b^a*Institute of Problems of Chemical Physics, Russian Academy of Sciences
142432, Chernogolovka, Moscow Region, Russia*^b*Joint Institute for High Temperatures, Russian Academy of Sciences
127412, Moscow, Russia*

Received March 10, 2008

The behavior of excess and intrinsic free electrons inside compressed inert gases is described as a function of pressure by using a pairwise approximation for the electron interaction with atomic surroundings. The change of sign from negative to positive for the xenon atom electric potential inside condensed xenon is predicted to occur at a pressure around 3 GPa, preventing slow electron embedding into solid xenon from the gas phase at higher pressure. To overcome this difficulty, the electrons should be injected into a solid sample just before its pulsed shock loading. The ionization of xenon by pressure and its further metallization are described by decreasing the forbidden gap at the account of increasing the xenon ground electronic term and simultaneous splitting the upper ionized electronic state. A good coincidence between calculated and measured pressure of the dielectric–metal transition in xenon is demonstrated.

PACS: 34.80.-i, 52.80.Wq, 52.80.Yr, 79.20.Kz

1. INTRODUCTION

When an excess electron is injected into a heavy condensed inert gas, this system becomes similar to a metal with respect to electron transport. Indeed, the mean free path of a slow excess electron in condensed argon, krypton, and xenon may be as large as several meters, and the electron mobility in these condensed systems is several times greater than that in metals [1]. Due to the smallness of the electron number density, this system is convenient for the study of metal properties in the absence of the electron–electron interaction and the electric field screening by space charge inherent to standard metals [2–4]. In particular, such an analysis shows [5] that excess electrons propagate inside condensed heavy inert gases along specific channels, the lines of the Voronoi–Delone net for this system.

These matrices are also suitable for experimental study [6–8]. Indeed, the electric potential for an electron inside dense inert gases is lower than that in the vacuum [1], and an electron freely penetrates dense inert gases from outside. The excess electrons inside a condensed inert gas can be governed by an external

electric field and can even excite the matrix, but ionization processes are absent there [9], in contrast to gases. Therefore, to organize an electric discharge in a condensed inert gas, it is necessary to provide the electron multiplication outside the matrix. This scheme of an electric discharge was realized in [10–12] by using the transformation of the exciton energy into the energy of emitted VUV photons and then into the secondary electron photoemission from a cathode. Because the efficiency of the electric field energy transformation into VUV light is about 20 %, this effect can be used for an effective generation of VUV photons. The fast excess electrons appearing inside the matrix can also induce various physical and chemical processes inside condensed inert gases.

The systems under consideration are known to be the most popular objects for studying the matter transformation at high and superhigh pressure. The dielectric–metal transition has been experimentally proved specifically for xenon [13–15] as proceeding at the pressure 130–140 GPa. The aim of this paper is to analyze the electric properties of condensed inert gases with and without excess electrons at high pressures from these standpoints.

*E-mail: gordon@ficp.ac.ru

2. EXCESS ELECTRONS INSIDE DENSE INERT GASES

In considering the conductivity of dense inert gases involving excess electrons, we deviate from the traditional scheme [16–21] that assumes the interaction of excess electrons inside inert gases to be a sum of interactions with individual atoms. This approach is valid only at low atom densities or at a high electric field. In our case of high electron mobilities, every electron interacts collectively with a system of surrounding atoms. Based on experimental data, we found [5] that electrons propagate through Voronoi–Delone channels [22, 23], which are found to exist between nearest atoms of a condensed inert gas. Indeed, in a rare inert gas, an electron is repulsed from an atom in the vicinity of the atom and is attracted to the atom at intermediate distances between atoms. Hence, there is an optimal density of a heavy inert gas [9] at which an electron prefers to be located between neighboring atoms.

The Voronoi–Delone channels are shown in Fig. 1 in the case where atoms of a condensed inert gas form a crystalline structure. We note that in reality, electrons are located in tubes around the Voronoi–Delone channels, and therefore the crystal structure is not mandatory for the electron free motion if the curvature of these tubes is sufficiently small. This character of electron conductivity in compressed inert gases is important for the analysis of these processes at high pressures.

Thus, in considering the collective character of the electron drift in condensed inert gases, we are based on two types of electron interaction with valent electrons of atoms. The first type of exchange interaction occurs if an electron penetrates inside an atom and is repulsed

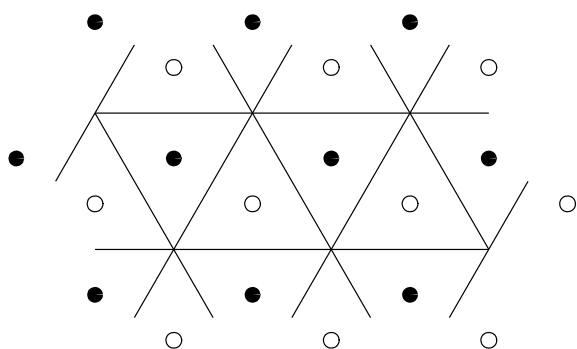


Fig. 1. Voronoi–Delone channels (solid lines) for propagation of an excess electron in a solid inert gas. Positions of atoms of a lower (open circles) and upper (solid circles) layer

Table 1. Parameters of the potential energy for an excess electron inside condensed inert gases

	Ar	Kr	Xe
$U_{min}, \text{ eV [24–27]}$	−0.33	−0.53	−0.77
$N_{min}, 10^{22} \text{ cm}^{-3}$	1.1	1.2	1.1
$C, \text{ eV}$	0.44	0.71	1.04
α	4	4	4
$A, \text{ eV}$	6	10	14
$N_{cr}, 10^{22} \text{ cm}^{-3}$	2.4	2.6	2.4

from there in accordance with the Pauli exclusion principle. The other type of the electron–atom interaction proceeds above the atom surface. In principle, the set of valent electrons can provide the interaction of different signs, but in the particular case of Ar, Kr, and Xe atoms, this electron–atom interaction is attractive. Based on the above consideration, we represent the interaction potential for an electron with a condensed rare gas as

$$U(N) = -C \frac{N}{N_{min}} + A \exp\left(-\alpha \frac{N_{min}}{N}\right), \quad (2.1)$$

where N is the current number density of atoms and N_{min} is the number density of atoms at which the interaction potential has a minimum. Of course, only the general form of the $U(N)$ dependence can be predicted this way, and therefore the parameters in (2.1) have to be determined from experimental data [5]; they are given in Table 1. We note that the value of this interaction potential is proportional to the electric potential for the electron placed in a condensed system. The maximum attraction of an electron inside an inert gas occurs at the number density N_{min} of atoms when the electric potential of the electron is equal to $-U_{min}/e$.

Figure 2 demonstrates the reliability of the electron energy presentation in form (2.1) with the example of Ar. As follows from (2.1), an electron can be attracted by xenon inside a condensed matter only in a limited range of the atom number densities. Table 1 contains the critical atom number density N_{cr} at which the electron energy becomes zero. For the atom number densities exceeding this value, the Voronoi–Delone mechanism of electron mobility is not valid because an excess electron does not experience attraction inside the inert gas anymore.

The existence of the critical atom number density N_{cr} is important for experiment. Indeed, until the elec-

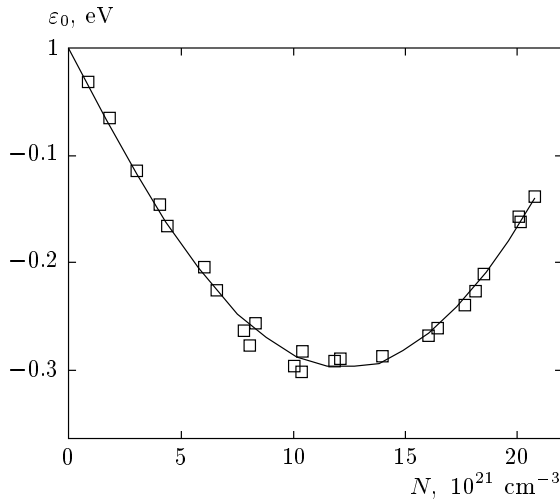


Fig. 2. The electron energy inside compressed argon. Small squares, — experiment [24]; solid curve, — formula (2.1)

tric potential inside an inert gas is below the potential in the vacuum, electrons penetrate this inert gas from outside freely, and electric discharge in a compressed inert gas may be arranged as it was arranged at ambient pressure. According to the data in Table 1, this possibility is lost at pressures of 3 GPa, which correspond to the molar volume 25 cm^3 . The mobility of an excess electron inside the solid starts decreasing long before that pressure is reached.

3. CONDUCTIVITY OF CONDENSED INERT GASES AT HIGH PRESSURES

At a much higher pressure, another conductivity mechanism of compressed inert gases can develop due to a dielectric–metal transition in this system [28]. From the general standpoint, this should happen for xenon compressed such that the distances between nearest neighbors become shorter than the distance between nuclei of the diatomic ion.

Indeed, the energy of the electron ground state increases due to a repulsive interaction between atoms, and the energy of the ionized state may decrease due to an attractive interaction between an atomic ion and surrounding atoms. Our goal is to find the pressure at which the energy gap separating the ground electron state of this system and its ionized state starts to significantly decrease and eventually disappears. The experimenters describe that effect as the “ionization by pressure”. In this consideration, we assume the pair interaction potential between neighboring atomic par-

ticles to be relatively small. This is justified by a large number (around 12) of the nearest-neighbor atoms.

As a condensed inert gas shrinks under the action of an external pressure, repulsion of nearest atoms due to overlapping of their electron shells increases. Because the exchange interaction potential of two atoms due to the overlap of their electron orbits is determined mainly by a region of electron coordinates near the axis that joins nuclei of the interacting atoms [29], the interaction should be close to the pairwise one; therefore, the interaction between two nearest atoms is almost independent of the positions of other atoms. Then the total interaction potential of a given atom is the sum of its interaction potentials with neighboring atoms.

We next express the change in the total electron energy ΔE of the atom ensemble depending on the atom configuration as

$$\Delta E = \frac{\langle \Psi | \hat{H} | \Psi \rangle}{\langle \Psi | \Psi \rangle},$$

where \hat{H} is the electron Hamiltonian and, in the one-electron approximation, the wave function Ψ of the total atom ensemble is expressed through the wave functions of electrons of individual atoms ψ_i as

$$\Psi = \prod_i \psi_i,$$

where ψ_i is the wave function of electrons for the i th atom.

We divide the Hamiltonian of electrons of a given system into the one-atom part \hat{h}_i and the two-atom part \hat{h}_{jk} ,

$$\hat{H} = \sum_i \hat{h}_i = \sum_{i \neq j, k} \hat{h}_i + \hat{h}_{jk}.$$

The two-atom part of the Hamiltonian includes the interaction between electrons of neighboring atoms. Taking only the exchange interaction for electrons belonging to different atoms into account, we find the total electron energy of this system as

$$\begin{aligned} \Delta E &= E_0 + n \frac{q}{2} \sum_{j, k} \frac{\langle \psi_j(1) \psi_k(2) | \hat{h}_{jk} | \psi_k(1) \psi_j(2) \rangle}{1 + \langle \psi_j(1) \psi_k(2) | \psi_k(1) \psi_j(2) \rangle} = \\ &= E_0 + n \frac{q}{2} U(R_0), \end{aligned} \quad (3.1)$$

where for simplicity the distances between nearest neighbors are assumed to be the same and equal to R_0 . Then q is the average number of nearest neighbors, $U(R)$ is the interaction potential for two atoms

Table 2. Parameters of the interaction potential for two xenon atoms in the range of their strong repulsion, where $U(R_0) = 1$ eV

	R_0	k
Experiment [30]	5.5	6.7
Experiment [31]	5.0	6.4
Theory [33, 34]	5.6	7.8

at the distance R between them, and n is total number of atoms. The summation in formula (3.1) ranges all the atoms and all the valence electrons of each atom.

Thus, we represent the interaction potential for an atom located inside a system of inert gas atoms under high pressure as a sum of the pair interaction potentials between nearest neighbors, and the pair interaction potentials are determined by exchange interactions, which are expressed through the overlap of the wave functions for electrons belonging to different atoms. As has already been stated, the exchange interaction of two atoms is assumed to be independent of their interaction with other atoms, and hence the total interaction potential can be represented as the sum of the pair interaction potentials. The factor one half in formula (3.1) accounts for the fact that each interaction involves two atoms.

At small distances, the pair interaction potential of two atoms with completed electron shells is determined by the overlapping of electron shells and leads to a strong repulsion of atoms. Hence, the repulsive interaction potential $U(R)$ of two atoms varies sharply with the distance R between atoms, and we approximate it by the dependence

$$U(R) = U(R_0) \left(\frac{R_0}{R} \right)^k, \quad k = \frac{d \ln U}{d \ln R}_{R=R_0}. \quad (3.2)$$

In what follows, we consider only xenon atoms because the electric properties of compressed xenon are better studied experimentally. Table 2 gives the parameters of the pair interaction potential of xenon atoms in a range where it is close to 1 eV. Experimental parameters [30–32] are determined from small-angle scattering measurements in a system of two xenon atoms, and the theoretical parameters [29, 33, 34] follow from the asymptotic theory that assumes distances between the interacting atoms to be sufficiently large, such that the interaction potential of atoms is small compared to the atom ionization potential. According to the asymptotic

theory [29, 33, 34], the exchange interaction potential of two atoms is given by

$$U(R) = A^4 F(\gamma) R^{7/2\gamma-1} \exp(-2R\gamma), \quad (3.3)$$

where $\gamma^2/2$ is the atom ionization potential, A is the asymptotic coefficient, and we use the atomic units $\hbar = m_e = e^2 = 1$; we note a confined accuracy of the asymptotic coefficient. In the case of xenon, these parameters are $\gamma = 0.944$ and $A = 2.0$, and the interaction potential is [29, 33, 34]

$$U(R) = 14R^{2.71} e^{-1.888R}. \quad (3.4)$$

The reliability of the experimental data and of their theoretical description can be seen from Table 2.

Thus, the main interaction in the ground electron state of condensed inert gases is due to the exchange interaction between valence electrons. Expressing this interaction potential through pair exchange interaction potentials between nearby atoms allows improving the accuracy of the data by conjugation of experimental and theoretical data. This interaction leads to a decrease in the ionization potential for a condensed inert gas. We see that under the adopted conditions, this value depends on the number of nearest neighbors of a given structure. Guided by the solid state of xenon, we note a nonuniform distribution of atoms there [35]. Indeed, this atomic system consists of individual clusters — domains in which the number of nearest neighbors is $q = 12$, while an average number of nearest neighbors is approximately $q = 10$. This implies that in the course of compression of inert gases, the gap between the ground electron state and the ionized state should disappear first inside the clusters, with the boundaries between them remaining isolators. Thus, the transition from the dielectric to the metal state has a complex character in compressed inert gases.

Along with an increase in the energy of the electron term of the ground state of condensed xenon, there is a decrease in the energy of the electron term for an ionized state. But the nature of this effect is different from that for the ground state. Indeed, on average, the electron term of the ionized state does not change under compression, but splits in energy, transforming into a band with its edges moving up and down. In what follows, we assume the steady distribution of atoms in the crystal in the interaction frame between nearest neighbors only. We additionally assume that the pressure is so high that the distances between an ion and surrounding atoms are identical to those between neighboring atoms. Under these conditions, we construct the electron terms of the ionized state. Evidently, due to

the exchange ion–atom interaction with nearest neighbors, each electron term of the ionized state splits into 12 electron terms. There is also an additional splitting of each of these terms due to translation symmetry along the crystal, but because this additional splitting is identical for all terms, we do not take this part of interaction into account.

We derive the wave function of the ionized state in the form

$$\Psi = \sum_i c_i \psi_i, \tag{3.5}$$

where ψ_i is the wave function describing an ion connected to the i th nucleus. Restricting ourselves by the interaction of a test nucleus with nearest neighbors only, we obtain 12 electron states with a different set of coefficients c_i , which are determined by the state symmetry. To find the minimal gap between the ionized and ground state, we find the term with the lowest energy. A test nucleus forms with its 12 nearest neighbors an octahedron; this geometric figure has the symmetry with respect to certain reflections and rotations of the frame of reference, and each operation leads to a certain transformation of the coefficients c_i in the expansion of the wave function. In the lowest electron state, these coefficients should be conserved under any symmetry operation. Hence, the wave function of this state has the form

$$\Psi = \sum_i c \psi_i, \tag{3.6}$$

and the coefficient c originates from the normalization condition. The corresponding negative energy shift per ion related to the symmetric lowest-energy state is

$$\begin{aligned} \Delta E &= \frac{\langle \Psi | \hat{H} | \Psi \rangle}{\langle \Psi | \Psi \rangle} = \\ &= \frac{q}{2} \frac{\langle \psi_i | \hat{h}_{ik} | \psi_k \rangle}{1 + \langle \psi_i | \psi_k \rangle} = \frac{q}{4} \Delta(R_0), \end{aligned} \tag{3.7}$$

where the wave function ψ_i means that the ion is connected to i th nucleus, R_0 is the average distance between nearest neighbors, and we reduced the change in the electron term of the ionized state to the pair exchange interaction potential $\Delta(R)$ for the interaction of the ion with the parent atom at a separation R . The exchange interaction potential between atoms i and k is here defined as

$$\begin{aligned} \Delta(R_{jk}) &= 2 \langle \psi_i | \hat{h}_{ik} | \psi_k \rangle - \\ &- 2 \langle \psi_i | \hat{h}_{ik} | \psi_i \rangle \langle \psi_i | \psi_k \rangle, \end{aligned} \tag{3.8}$$

where \hat{h}_{ik} is the one-electron Hamiltonian describing the electron located in the field of two nuclei. The above expression is valid at large distances between nuclei when the overlap of the wave functions centered on different cores is not large.

We recall that in contrast to the single-electron term of the ground state, we have in this case the number of electron terms coincident with the number of nuclei. These electron terms are concentrated with respect to energy into separate groups. The number of such groups is approximately equal to the number of nearest neighbors, and their energies differ remarkably. Formula (3.7) relates to the lowest electron term of the symmetric state. Only this state is interesting to us because it opens the shortest route for the electron passage from the ionized to ground state, i.e., for atom ionization. Eventually, the intersection of electron terms related to the ionized and ground states of the atom system leads to the dielectric–metal transition.

We use formula (3.7) in the particular case of the interaction of an ion with the parent atom. Setting $q = 1$, we obtain the electron energy

$$\varepsilon_g = -\frac{1}{2} \Delta(R), \tag{3.9}$$

where R is the distance between the nuclei. There are two electron terms in this case, even (gerade g) and odd (ungerade u) ones, and if we account for the exchange interaction only, the energies of these states are

$$\varepsilon_g = -\varepsilon_u = -\frac{1}{2} \Delta(R). \tag{3.10}$$

This means that the gerade (even) electron term goes down, the ungerade (odd) electron term goes up, and the splitting of these terms $\varepsilon_g - \varepsilon_u$, the exchange interaction potential, is $\Delta(R)$.

For xenon, it is important that the exchange interaction potential depends on the angular momentum projection for a p -electron transferring valence. With the angle between the axis that joins the interacting atoms and the quantization axis on which the angular momentum projection for a transferring p -electron is zero denoted by θ , the exchange interaction potential of an ion and the parent atom is given by [29, 33, 36]

$$\Delta(R) = 3\Delta_0(R) \cos^2 \theta, \tag{3.11}$$

where $\Delta_0(R)$ is the exchange interaction potential for a transferring s -electron with the same asymptotic parameters. Averaging over the angle θ and assuming the nearest neighbors to be located in different directions, we obtain

$$\Delta E = \frac{q}{4} \Delta_0(R_0), \tag{3.12}$$

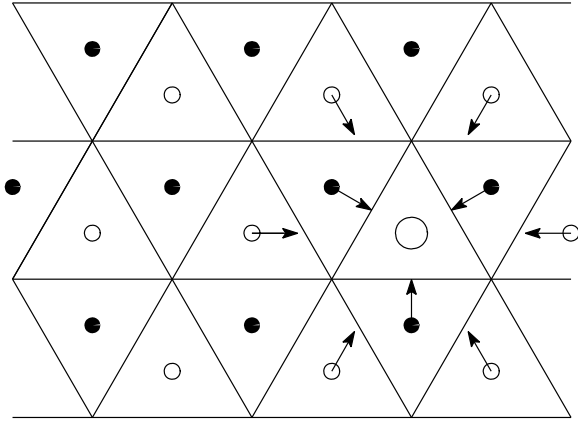


Fig. 3. Displacement of atoms near a forming ion

where R_0 is the average distance between nearest neighbors. In the framework of the asymptotic theory [29, 33, 36], the expression for the exchange interaction potential for an ion with the parent atom is equal to

$$\Delta(R) = A^2 R^{2/\gamma-1} \exp(-R\gamma - 1/\gamma). \quad (3.13)$$

Correspondingly, the exchange interaction potential of a xenon atom and an ion is equal to

$$\Delta(R) = 1.4R^{1.12} \exp(-0.944R) \quad (3.14)$$

in atomic units.

Let R_* be the average distance between the nearest neighbors corresponding to the intersection of electron terms belonging to the ground state of repulsing atoms and to the ionized state. This value follows from the equation

$$J = \frac{q}{2}U(R_*) + \frac{q}{4}\Delta(R_*), \quad (3.15)$$

where J is the atom ionization potential, $U(R)$ is the repulsive interaction potential at a distance R for two atoms due to their exchange interaction, $\Delta(R)$ is the exchange interaction potential of an ion with its parent atom, and q is the number of nearest atoms. In principle, we should include the terms describing the interactions of the formed ion and the electron with xenon surroundings into this equation. The energy of the ion is determined by the displacement of Xe atoms in the direction to the ion as is shown in Fig. 3. This energy is negative and cannot be significant in the rigid matrix of compressed xenon. The energy of the electron inside compressed xenon at the pressure of interest is positive because the number density of atoms N then exceeds N_{cr} in Table 1. Hence, the contributions to

Table 3. The distance R_* between nearest neighbors corresponding to the dielectric–metal transition in xenon, the atom number density N_* , and the molar volume V_*

	R_*, a_0	$N_*, 10^{22} \text{ cm}^{-3}$	$V_*, \text{ cm}^3/\text{mol}$
Case 1	5.16	5.8	10
Case 2	5.15	5.8	10
Case 3	5.29	5.4	11

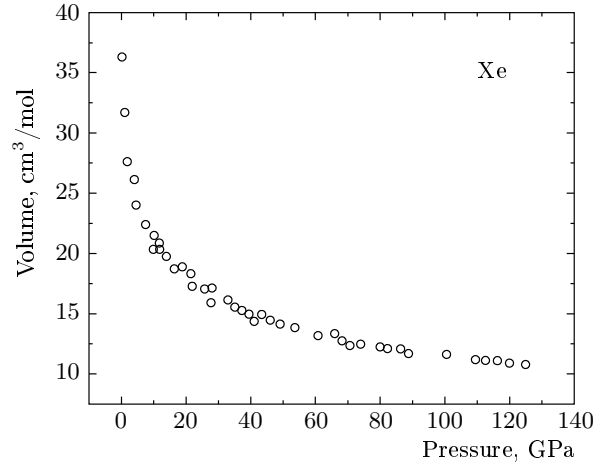


Fig. 4. The equation of state for xenon at high pressures according to the experiment in [37]

the energy from the electron and the ion have different signs and compensate each other. Because each of them is less than 1 eV, their inclusion is not significant in any case because the sum of the two leading terms in (3.15) exceeds 10 eV.

The data in Table 3 are the results of using the parameters of the atom–atom interaction in Table 1 and formulas (3.12) and (3.14) for the exchange ion–atom interaction potential of xenon. In cases 1 and 2, we use the experimental data in [30] and [31, 32] for the pair interaction potential of two xenon atoms, and in case 3, we use formula (3.4) [33, 34]. As can be seen, the number density of atoms N_* for the dielectric–metal transition is approximately twice the critical atom number density N_{cr} for the Voronoi–Delone mechanism of electron drift.

To pass from the molar volume V to the pressure p measured in experiment, we need the Xe equation of state valid at high pressure. Figure 4 gives the equation of state for compressed xenon measured up to the range of the dielectric–metal transition. According to

it, the molar volume at the dielectric–metal transition for xenon $V_* = 10\text{--}11 \text{ cm}^3/\text{mol}$ corresponds to the pressure 120–140 GPa, which nicely fits the experimental results in [13, 14, 15].

4. CONCLUSION

The aim of this analysis was to describe the changes in the behavior of a free electron embedded into condensed inert gases at high and extrahigh pressure, to reveal the connection of their characteristics with the structure of solids, and to develop the strategy for experimentally studying the mobility and conductivity of excess and intrinsic electrons in solid xenon. It was shown, in particular, that under the pressure exceeding 3 GPa, the slow electrons cannot be embedded into solid xenon from the gas. Thus, the approach has been proposed for the blasting experiments when the electrons are introduced into the xenon crystal at ambient pressure, and then the sample is subjected to a shock wave action. Because shock loading lasts less than 1 microsecond and the electron lifetime in a sample is 3 microseconds, there is enough time for measurements.

The special attention has been devoted to understanding the nature of xenon metallization at high pressure. As a matter of fact, the absolute value of xenon molar volume corresponding to the dielectric–metal transition was predicted with good accuracy by exclusively using the characteristics of atom–atom and electron–atom interactions obtained theoretically or in the experimental study of elementary processes in the gas. If the proposed interpretation of the “ionization by pressure” is correct, the whole dependence of the forbidden electron band on pressure for any condensed heavy inert gas can be readily found, and, in particular, the pressures of the dielectric–metal transition for at least argon and krypton can be predicted.

This work is supported in part by the RFBR (grant № 07-03-00393). The authors are thankful to P. V. Kashtanov for some numerical calculations.

REFERENCES

1. B. M. Smirnov, *Uspekhi Fiz. Nauk* **172**, 1411 (2002).
2. N. W. Ashcroft and N. D. Mermin, *Solid State Physics*, Holt, Rinehart and Winston, New York (1976).
3. Ch. Kittel, *Introduction to Solid State Physics*, Wiley, New York (1986).
4. P. M. Chaikin and T. C. Lubensky, *Principles of Condensed Matter Physics*, Cambridge Univ. Press, Cambridge (1995).
5. E. B. Gordon and B. M. Smirnov, *Zh. Eksp. Teor. Fiz.* **128**, 211 (2005).
6. E. B. Gordon, O. S. Rzhavsky, and V. V. Khmelenko, *Quant. Electr.* **21**, 227 (1994).
7. E. B. Gordon, V. V. Khmelenko, and O. S. Rzhavsky, *Chem. Phys. Lett.* **217**, 605 (1994).
8. E. B. Gordon and A. F. Shestakov, *Low Temp. Phys.* **27**, 883 (2001).
9. E. B. Gordon and B. M. Smirnov, *Zh. Eksp. Teor. Fiz.* **125**, 1058 (2004).
10. E. B. Gordon, G. Frossati, and A. Usenko, *Zh. Eksp. Teor. Fiz.* **123**, 846 (2003).
11. A. Usenko, G. Frossati, and E. B. Gordon, *Phys. Rev. Lett.* **90**, 153201 (2003).
12. E. B. Gordon, T. Kumada, M. Ishiguro, and Ya. Aratono, *Zh. Eksp. Teor. Fiz.* **126**, 898 (2004).
13. K. A. Goettel, J. H. Eggert, and I. F. Silvera, *Phys. Rev. Lett.* **62**, 665 (1989).
14. R. Reichlin, K. E. Brister, A. K. McMahan et al., *Phys. Rev. Lett.* **62**, 669 (1989).
15. M. I. Eremets, E. A. Gregoryanz, V. V. Struzhkin et al., *Phys. Rev. Lett.* **85**, 2797 (2000).
16. J. Lekner, *Phys. Rev.* **158**, 130 (1967).
17. M. H. Cohen and J. Lekner, *Phys. Rev.* **158**, 305 (1967).
18. B. E. Springett, J. Jortner, and M. H. Cohen, *J. Chem. Phys.* **48**, 2720 (1968).
19. V. M. Atrazhev and I. T. Iakubov, *J. Phys. C: Sol. St. Phys.* **14**, 5139 (1981).
20. V. M. Atrazhev and E. G. Dmitriev, *J. Phys. C: Sol. St. Phys.* **18**, 1205 (1985).
21. V. M. Atrazhev, I. V. Chernysheva, and T. D. Doke, *Jpn. J. Appl. Phys.* **41**, 1572 (2002).
22. B. N. Delone, *Uspekhi Math. Nauk* № 3, 16 (1937).
23. N. N. Medvedev, *The Voronoi–Delone Method in Studies of Structures of Noncrystal Systems*, Siberian Branch RAS Press, Novosibirsk (2000).
24. A. K. Al-Omari, K. N. Altmann, and R. Reiniger, *J. Chem. Phys.* **105**, 1305 (1996).

25. R. Reiniger, U. Asaf, and I. T. Steinberg, *Chem. Phys. Lett.* **90**, 287 (1982).
26. R. Reiniger, U. Asaf, and I. T. Steinberg, *Phys. Rev. B* **28**, 3193 (1983).
27. R. Reininger, U. Asaf, I. T. Steinberger et al., *Phys. Rev. B* **28**, 4426 (1983).
28. V. E. Fortov, V. Ya. Ternovoi, M. V. Zhernokletov et al., *Zh. Eksp. Teor. Fiz.* **124**, 288 (2003).
29. B. M. Smirnov, *Physics of Atoms and Ions*, Springer, New York (2003).
30. I. Amdur and J. E. Jordan, *Adv. Chem. Phys.* **10**, ch. 2, 29 (1966).
31. V. B. Leonas, *Uspekhi Fiz. Nauk* **107**, 29 (1972).
32. V. B. Leonas, in *Review of Science and Technology: Atomic and Molecular Physics*, ed. by S. A. Losev, VINITI, Moscow (1980), Vol. 1, p. 206.
33. B. M. Smirnov, *Asymptotic Methods in the Theory of Atomic Collisions*, Atomizdat, Moscow (1972) (in Russian).
34. B. M. Smirnov, *Uspekhi Fiz. Nauk* **162**(12), 97 (1992).
35. R. S. Berry and B. M. Smirnov, *Uspekhi Fiz. Nauk* **175**, 367 (2005); *Phys. Rev. B* **72**, 051510-1 (2005).
36. B. M. Smirnov, *Uspekhi Fiz. Nauk* **171**, 233 (2001).
37. H. Cynn, C. S. Yoo, B. Baer et al., *Phys. Rev. Lett.* **86**, 4552 (2001).